Istituto Nazionale di Fisica Nucleare
Sezione di Bologna

INFN/AE-74/1
28 Febbraio 1974

D. Banzi, E. Castelli[x], G. Giacomelli[o], F. Griffiths[+], A.A. Hirata[+][x], R. Jennings[+], P. Lugaresi-Serra, G. Mandrioli, C. Omero[x], A.M. Rossi and B.C. Wilson[+][-]: A STUDY OF 27940 τ^+ DECAYS IN FLIGHT. -

ABSTRACT. -

An Analysis has been made of 27940 $K^+ \longrightarrow \pi^+\pi^+\pi^-$ decays in flight, measured in the Saclay 81 cm bubble chamber filled with hydrogen or deuterium. After corrections for detection efficiency and Coulomb final state interaction, the Dalitz plot in the X, Y variables has been fitted to various X, Y dependences. The distributions are well represented with a form $(1+aY)$ with $a = 0.236 \pm 0.013$. The comparison with published data shows overall agreement and no evidence for CP violation.

(x) - Università di Trieste, and INFN, Sezione di Trieste.
(o) - And University of Padova, Padova, Italy.
(+) - University of Glasgow, Scotland.
(x) - Now at Physics Dept., University of Purdue, USA.
(-) - Now at Physics Dept., Royal Marsden Hospital, Sutton, Surrey, England.

1. - INTRODUCTION. -

In the course of a series of K^+p and K^+d experiments at laboratory momenta below 1.5 GeV/c[1-4] in the Saclay 81 cm bubble chamber we have measured over 30.000 τ^+ decays. The τ^+ were measured routinely for beam flux determination. At the end of the experiment we have collected these decays, and after appropriate selections we ended up with a clean sample of 27940 τ^+ decays. This statistics is comparable to that found in other bubble chamber experiments.

It may be interesting to remark that the first analysis of τ-decays included 13 events; now a standard bubble chamber experiment yields several tens of thousands of events, simply as a routine measurement of beam flux, while specialized counter experiments yield millions of events. On the other hand the simple picture on τ-decay which emerged from the study of the first few thousand events has not been significantly changed from the analyses of much larger samples. In particular the deviation from phase space seems to be adquately represented by a linear function of the Y variable. The slope of the function is equal for τ^+ and τ^- decays, consistent with CP conservation. The ratios of slopes for $\tau^{\pm}(K^{\pm} \to \pi^{\pm} \pi^+ \pi^-)$ $\tau'(K^{\pm} \to \pi^{\pm} \pi^0 \pi^0)$ and $K^0_L \to \pi^+ \pi^- \pi^0$ decays is consistent with a dominant I = 1/2 amplitude.

Section 2 of this paper describes the experimental procedure and the corrections applied to the data. The results are discussed in Section 3 and are compared with the results of the literature.

2. - EXPERIMENTAL. -

The 81 cm Saclay bubble chamber filled with either hydrogen or deuterium was exposed at the CERN proton synchrotron to electrostatically separated K^+ beams with momenta below 1.5 GeV/C. About 800.000 pictures from a number of different experiments were analyzed for $K^+ \to$ $\to \pi^+ \pi^+ \pi^-$ decays in flight, yielding over 30.000 events. Details of the exposures can be found in references (1-4).

Most of the film was scanned twice for three-prong events, yielding an overall scanning efficiency of 96% for a single scan and 99% for a double scan. Events with obvious electron tracks were removed from the sample.

Measurement were done on Mangiaspago machines in Bologna and Trieste and on SMP machines in Glasgow. Measured events were processed through either the CERN THRESH-GRIND-SLICE or the Rutherford Laboratory GEOMETRY-KINEMATICS chain of programs for geometrical reconstruction and kinematics fitting. All events failing at any stage were remeasured at least once. The failing events were checked at the scanning table to discriminate between τ-decays, decays involving electrons and K^+ interac-

tions. τ^+-decays were defined as such if they fitted the τ^+ hypothesis with a probability larger than 0.1%. 27940 events satisfied the criteria inside the fiducial volume of the chamber. The number of events according to primary K^+ momentum and bubble chamber fillings are listed in Table I.

TABLE I

List of τ^+-events according Kaon Laboratory momentum and bubble chamber filling.

Kaon Laboratory momentum (GeV/c)	Bubble chamber filling	Number of events
0.145	Hydrogen	287
0.175	"	557
0.200	"	859
0.250	"	2841
0.300	"	899
0.340	"	836
0.370	"	164
0.410	"	40
0.78	"	3030
0.90-1.45	"	4771
0.64	Deuterium	1403
0.72	"	1570
0.78	"	946
0.85	"	1870
0.90	"	1250
0.98	"	660
1.06	"	1404
1.13	"	650
1.21	"	1310
1.29	"	400
1.35	"	1146
1.42	"	697
1.51	"	350
Total number of τ		27.940

A comparison of the measured pion momentum distribution in the laboratory frame with that from a Montecarlo calculation, showed that below 400 MeV/c we were missing 50-70% of the events with a pion momentum smaller than 30 MeV/c, corresponding to range smaller than 0.5 cm. Thus at primary momenta below 400 MeV/c a cut was made to eliminate from the sample those events in which the momentum of any pion was smaller than 30 MeV/c. The cut removed 120 events. The remaining events were each weighted by a factor $w_1 = 1/(1-p)$, where p is the probability that any one pion has a laboratory momentum smaller than 30 MeV/c. The probability p and the weight w_1 were computed by means of the Montecarlo program as ratios of events, in each bin of the Dalitz plot, with and without the cut. p and thus w_1 are a function of the incident momentum and of the location of the event in the Dalitz plot. Table II gives the weight w_1 at $p_{lab} = 250$ MeV/c.

TABLE II

Weight factors for the loss of low momentum pions at an incident Kaon laboratory momentum of 0.25 GeV/c.

0.872	1.08	1.08	1.07	1.06	1.04					
0.776	1.09	1.09	1.08	1.07	1.05	1.02	1.01			
0.680	1.10	1.09	1.08	1.07	1.06	1.03	1.01	1.00		
0.584	1.10	1.09	1.08	1.07	1.06	1.04	1.02	1.00	1.00	
0.488	1.09	1.08	1.08	1.07	1.06	1.05	1.02	1.00	1.00	1.00
0.392	1.09	1.08	1.08	1.08	1.07	1.05	1.03	1.01	1.00	1.00
0.296	1.09	1.08	1.08	1.08	1.07	1.06	1.04	1.02	1.01	1.01
0.200	1.09	1.08	1.08	1.08	1.08	1.07	1.06	1.04	1.02	1.01
0.104	1.09	1.09	1.09	1.09	1.08	1.08	1.07	1.05	1.04	1.02
0.008	1.09	1.09	1.09	1.09	1.09	1.09	1.08	1.06	1.05	1.03
-0.088	1.09	1.09	1.09	1.09	1.09	1.09	1.08	1.07	1.06	1.05
-0.184	1.09	1.09	1.09	1.09	1.09	1.09	1.09	1.09	1.08	1.06
-0.280	1.09	1.09	1.09	1.09	1.09	1.10	1.10	1.10	1.09	1.06
-0.376	1.08	1.08	1.08	1.09	1.09	1.10	1.10	1.09	1.09	
-0.472	1.08	1.08	1.08	1.08	1.08	1.09	1.09	1.09	1.09	
-0.568	1.07	1.07	1.07	1.07	1.08	1.08	1.09	1.09		
-0.664	1.05	1.05	1.06	1.06	1.07	1.07	1.08	1.09		
-0.760	1.02	1.03	1.03	1.04	1.05	1.06	1.07			
-0.856	1.00	1.01	1.01	1.02	1.03					
-0.952	1.00	1.01	1.01	1.01						
Y/X	.048	.144	.240	.336	.432	.528	.624	.720	.816	.912

No correction was required for the data at Kaon momenta above 600 MeV/c.

Coulomb correction. In order to compare spectra of various charged modes of K-decays and to compare with theoretical weak interactions predictions, the experimental spectra have to be corrected for the effects of final state Coulomb interactions. The two pions with equal charge will repel each other and will thus favous configurations of larger relative velocities, while pions of opposite sign attract each other and favour configurations of lower relative velocities. Different authors use slightly different Coulomb corrections. We shall use the form proposed by Dalitz[5-7]: Each measured event has been divided by a weight factor:

(1) $$W = W_{12} W_{13} W_{23} = \frac{Z_{12}}{e^{Z_{12}} - 1} \quad \frac{Z_{13}}{e^{Z_{13}} - 1} \quad \frac{Z_{23}}{e^{Z_{23}} - 1}$$

where

(2) $$Z_{ij} = 2 \pi \alpha \frac{e_i e_j}{\beta_{ij}}$$

α = (fine structure constant) = $\frac{1}{137.036}$

e_i, e_j = pion charges in units of e

β_{ij} = (relative π_i, π_j velocities in units of c) = $\left| \frac{\vec{P}_i}{E_i} - \frac{\vec{P}_j}{E_j} \right|$

The distribution of these weight factors over the Dalitz plot is shown in Table III.

The final three-pion system is described by nine parameters; the four equations of energy-momentum conservation reduce them to five independent variables, which may be chosen to be, for instance, five angles. Three angles, two of which determine the orientation in space of the decay plane and the third the direction of the first pion in the plane, may be ignored, because of the absence of spin effects. We are thus left with two variables only. Different choices are found in the literature. We have chosen the Dalitz variables X and Y defined as:

(3) $$X = \frac{\sqrt{3}}{Q} |T_1 - T_2|$$

TABLE III

Coulomb weights as function of X and Y.

-0.872	0.975	0.976	0.987	0.997	1.002					
0.776	1.007	1.007	1.008	1.009	1.009	1.010	1.010			
0.680	1.015	1.015	1.015	1.015	1.015	1.016	1.017	1.018		
0.584	1.018	1.019	1.019	1.019	1.020	1.020	1.022	1.022	1.022	
0.488	1.020	1.021	1.022	1.022	1.022	1.022	1.023	1.024	1.026	1.028
0.392	1.022	1.023	1.023	1.023	1.023	1.024	1.025	1.026	1.027	1.029
0.296	1.024	1.025	1.025	1.025	1.026	1.026	1.027	1.027	1.029	1.032
0.200	1.025	1.026	1.026	1.026	1.027	1.028	1.028	1.029	1.032	1.035
0.104	1.026	1.027	1.027	1.027	1.028	1.029	1.030	1.032	1.034	1.038
0.008	1.027	1.028	1.028	1.028	1.029	1.030	1.032	1.034	1.037	1.044
-0.088	1.028	1.029	1.029	1.029	1.030	1.031	1.034	1.036	1.041	1.050
-0.184	1.029	1.030	1.030	1.031	1.032	1.033	1.036	1.041	1.046	1.065
-0.280	1.030	1.030	1.031	1.032	1.034	1.035	1.039	1.044	1.060	1.090
-0.376	1.031	1.031	1.032	1.033	1.035	1.037	1.041	1.051	1.098	
-0.472	1.032	1.032	1.033	1.034	1.036	1.039	1.046	1.067	1.195	
-0.568	1.033	1.034	1.034	1.036	1.039	1.044	1.057	1.103		
-0.664	1.034	1.035	1.036	1.038	1.042	1.048	1.068	1.111		
-0.760	1.035	1.036	1.038	1.040	1.046	1.055	1.075			
-0.856	1.036	1.037	1.039	1.042	1.048	1.070				
-0.952	1.038	1.039	1.042	1.043						
Y/X	0.048	0.144	0.240	0.336	0.432	0.528	0.624	0.720	0.816	0.912

(4) $$Y = \frac{1}{Q}(3T_3 - Q)$$

where T_1, T_2 and T_3 are c.m. kinetic energies. Q is the c.m. kinetic energy available for the three pions:

(5) $$Q = m_k - 3m_\pi = T_1 + T_2 + T_3$$

For $\tau^{\pm}$-decays the ranges of variability of X and Y are the following:

(6) $$0 \leq X \leq 0.965, \qquad -1 \leq Y \leq 0.924$$

The equation which gives the limiting contour in the (X, Y) plane is :

(7) $$X = \left\{ (Y+1) \frac{\left[\frac{Q}{3}(Y+1)+2m_\pi\right]\left[m_k + m_\pi - \frac{2}{3}m_k(Y+1)\right]}{(m_k - m_\pi)^2 - \frac{2}{3}m_k Q(Y+1)} \right\}^{1/2}$$

3.- RESULTS AND DISCUSSION.-

Table IV give the array of the events over the Dalitz plot. The events have been weighted for the low-momentum-pion cut and for final--state Coulomb interactions. The statistical error on each of these points is approximately equal to the square root of the number of events. The number of events projected on the X and Y axis are given in Table IV and are shown in Figure 1 and 2, where they are compared with the predictions of phase space (solid line).

The X-distribution follows rather closely the prediction of phase space, while the Y distribution deviates considerably, with a concentration of events towards large positive values of Y and a corresponding depletion at large negative values of Y.

These deviations are better seen in Figures 3, 4 and in Tables V, VI which give the values of the matrix element squared, $|M|^2$, versus X and Y. $|M|^2$ is defined as

(8) $$|M|^2 \propto \frac{\text{number of events}}{\text{phase space}}$$

Fig. 3 shows that in reality there is a slight deviation of the X-distribution from phase space and thus $|M|^2$ is not quite a constant function of X. The Y-distribution (see Fig. 4) deviates linearly from phase space. More quantitative information may be obtained by fitting the array of events over the

TABLE IV

Dalitz plot distribution of events after corrections for the loss of low momentum pions and for final-state Coulomb interactions. The statistical error on each data point is approximately equal to the square root of the number of events.

0.872	236.9	209.9	168.7	116.6	58.4	1.0					791
0.776	210.5	193.9	208.1	216.4	203.8	155.0	41.0				1229
0.680	239.7	196.8	200.1	203.7	200.2	212.7	201.9	67.0	1.0		1523
0.584	182.1	215.3	187.0	195.2	211.0	212.8	166.9	205.2	88.2		1664
0.488	214.3	202.1	189.1	201.9	212.9	192.3	191.6	174.5	151.2	19.5	1749
0.392	205.3	162.1	181.5	202.4	214.1	179.4	206.5	156.4	172.1	82.7	1762
0.296	195.9	181.6	193.5	160.5	189.1	183.3	179.8	182.9	179.5	156.7	1803
0.200	203.6	169.3	174.2	207.5	177.9	172.5	177.2	185.5	171.4	163.6	1803
0.104	184.2	216.0	186.3	165.0	174.1	173.7	154.3	179.1	154.7	168.3	1756
0.008	183.9	182.9	141.3	157.1	164.0	184.3	157.6	172.4	146.5	173.9	1664
-0.088	174.7	173.2	170.3	171.3	144.4	179.1	189.8	170.9	182.0	125.8	1681
-0.184	149.8	185.9	149.7	153.4	171.1	172.6	170.6	163.4	147.6	89.9	1554
-0.280	145.6	156.5	166.0	169.5	153.6	165.9	160.8	151.8	187.7	27.0	1484
-0.376	162.0	165.7	175.1	183.7	150.3	152.8	178.4	146.6	129.0		1444
-0.472	154.7	167.4	143.7	153.6	150.0	130.6	147.7	141.3	45.2		1234
-0.568	153.9	161.7	161.1	127.8	146.9	174.9	133.8	82.1			1142
-0.664	145.1	149.1	156.7	143.3	150.9	136.9	119.6	13.7			1015
-0.760	122.4	153.4	131.9	145.1	148.1	124.1	21.5				846
-0.856	141.9	152.4	131.3	134.5	101.6	3.7					665
-0.952	113.9	120.4	62.8	17.3							314
	3520	3516	3278	3226	3122	2908	2599	2193	1756	1007	
Y/X	0.048	0.144	0.240	0.336	0.432	0.528	0.624	0.720	0.816	0.912	

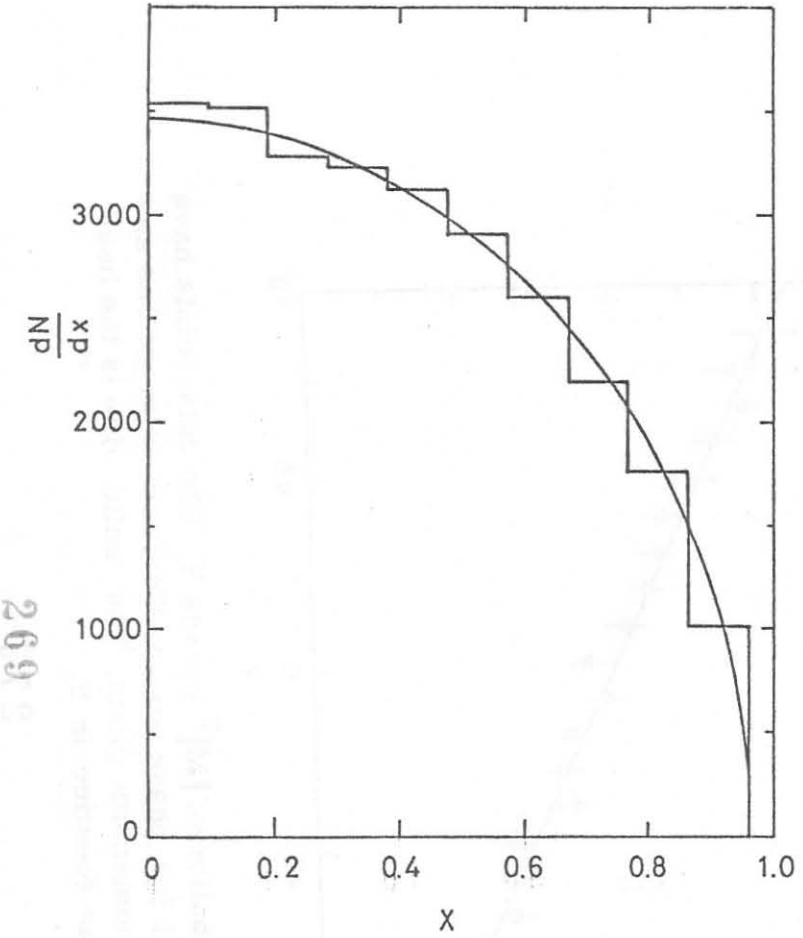

FIG. 1 - Distribution of the events in X compared to the prediction of relativistic phase space.

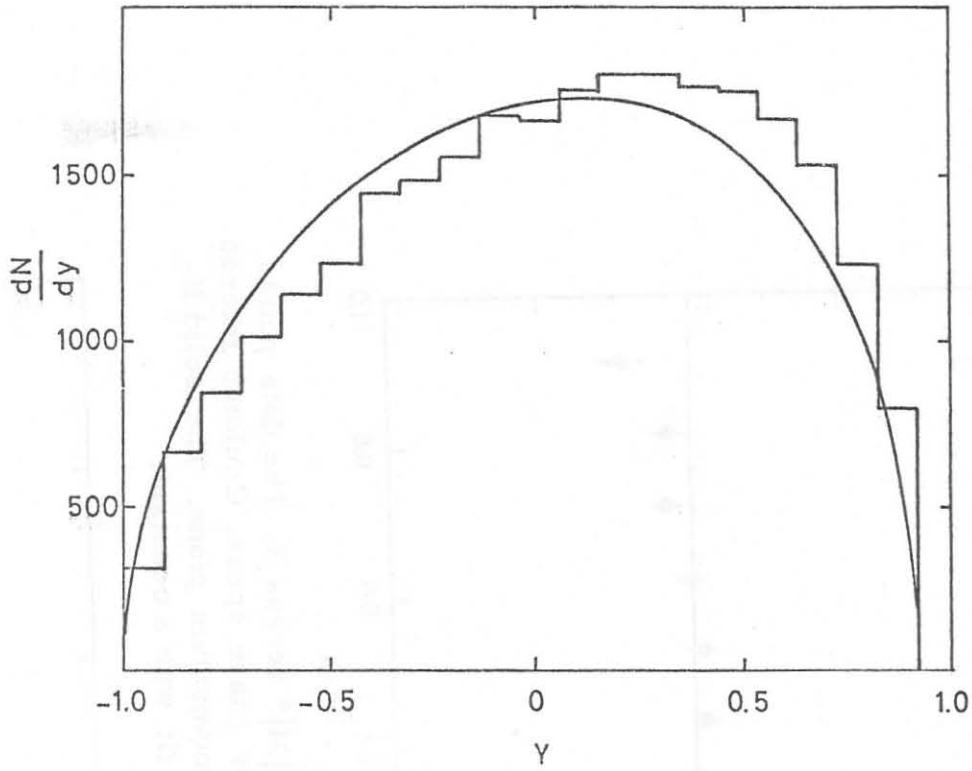

FIG. 2 - Distribution of the events in Y compared to the prediction of relativistic phase space.

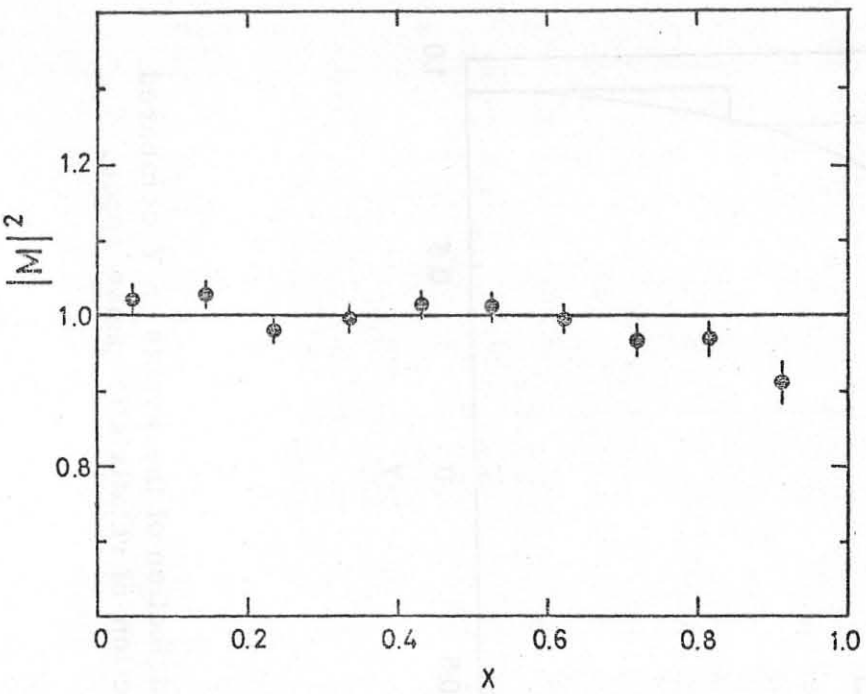

FIG. 3 - Distribution of $|M|^2$ versus X. The data points have been weighted for phase space, Coulomb interactions and a cut on low-momentum pions. The solid line represents the best fit with a constant.

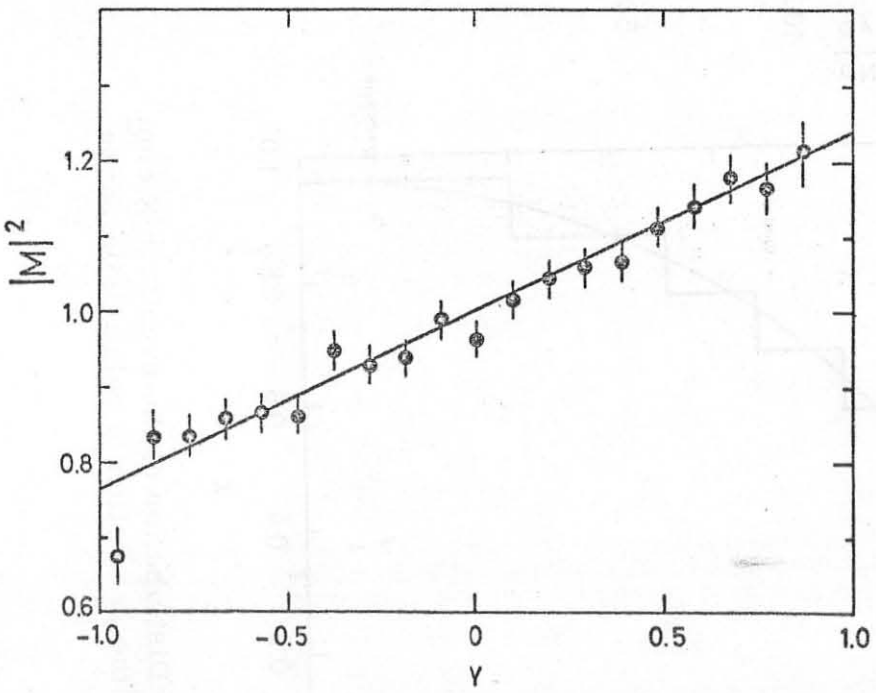

FIG. 4 - Distribution of $|M|^2$ versus Y. The data points have been weighted for phase space, Coulomb interactions and a cut on low momentum pions. The solid line is the best fit with a linear function in Y.

TABLE V

The number of events in $\Delta X = 0.096$ and $|M|^2$ as function of the X variable.

X	DN/DX	M^2
0.048	3520.4	1.022 ± 0.018
0.144	3515.6	1.030 ± 0.018
0.240	3278.4	0.981 ± 0.018
0.336	3225.8	0.998 ± 0.019
0.432	3122.4	1.015 ± 0.019
0.528	2907.6	1.014 ± 0.020
0.624	2599.0	0.998 ± 0.021
0.720	2192.8	0.969 ± 0.023
0.816	1756.1	0.974 ± 0.026
0.912	1007.4	0.931 ± 0.035

TABLE VI

The number of events in $\Delta Y = 0.096$ and $|M|^2$ as function of the Y variable.

Y	DN/DY	M^2
0.872	791.5	1.225 ± 0.048
0.776	1228.7	1.173 ± 0.036
0.680	1523.1	1.183 ± 0.037
0.584	1663.7	1.146 ± 0.030
0.488	1749.4	1.117 ± 0.027
0.392	1762.5	1.072 ± 0.026
0.296	1802.8	1.063 ± 0.026
0.200	1802.7	1.047 ± 0.025
0.104	1755.7	1.019 ± 0.025
0.008	1663.9	0.967 ± 0.024
-0.008	1681.5	0.993 ± 0.025
-0.184	1554.0	0.941 ± 0.024
-0.280	1484.4	0.932 ± 0.025
-0.376	1443.6	0.952 ± 0.026
-0.472	1234.2	0.886 ± 0.025
-0.568	1142.2	0.870 ± 0.026
-0.664	1015.3	0.863 ± 0.028
-0.760	846.5	0.840 ± 0.031
-0.856	665.4	0.842 ± 0.035
-0.952	314.4	0.686 ± 0.044

Dalitz plot (Table IV) divided by phase space with functions of the type

$$|M|^2 = 1 + aY + bY^2 + cX^2 + dX^4 + eX^2Y + fY^3 + \ldots . \tag{9}$$

Various types of fits, performed by setting some of the coefficients equal to zero, are given in Table VII for this and other experiments.

From an analysis of the fits of Table VII one may conclude that a linear dependence in Y, that is

$$|M|^2 = 1 + a\,Y \tag{10}$$

is an adequate representation of both τ^+ and τ^- Dalitz plots.

In compiling the results of the analyses of various authors one may phase the difficulty connected with a different choice of variables. Besides the form (10), the matrix element is written as[28]:

$$|M|^2 = 1 + g\,\frac{s_3 - s_o}{m^2_{\pi^+}} \tag{11}$$

$$= 1 + 2\,\alpha\,\frac{m_K}{m^2_{\pi^+}}\,(2T_3 - T_o) \tag{12}$$

where $m^2_{\pi^+}$ has been introduced to make the coefficients g and α dimensionless and

$$s_i = (P_k - P_i)^2 = (m_k - m_i)^2 - 2m_k T_i \tag{13}$$

$$s_o = \frac{1}{3}\sum_i s_i = \frac{1}{3}(m_k^2 + m_1^2 + m_2^2 + m_3^2) \tag{14}$$

The P_i are 4-vectors; m_i and T_i are mass and kinetic energy of the i-th pion; $i = 1, 2, 3$; the index 3 is used for the odd pion. $T_o = T_3$ max is the maximum value of T_3.

The relations among the "slopes" a, g and α are:

i) between g and a:

$$g = \frac{x_1\,a}{1 + y_1\,a} \tag{15}$$

TABLE VII

Results of various types of fits according to eq. (9).

	Events	Reference	a	b	c	d	e	f	x^2/DoF
τ^+	27.940	This exp.(x)	0.272 ±0.018	0.036±0.023	-0.056±0.067	-0.011±0.109	-0.183±0.081	-	1.07
	27.940	This exp.	0.268 ±0.017	-	-	-	-0.196±0.078	-	1.11
	27.940	This exp.	0.236 ±0.013(+)	-	-	-	-	-	0.89
	27.940	This exp.	0.240 ±0.013	-	-	-	-	-	1.14
	27.940	This exp.	0.254 ±0.031	0.039±0.021	-0.064±0.021	-	-0.163±0.090	0.034±0.065	1.06
τ^-	51.000	Mast (13)	0.244 ±0.013	-0.002±0.020	-0.067±0.060	0.069±0.083	0.023±0.054	-	1.09
τ^+	750.000	Ford (15)	0.2734±0.0035	0.030±0.010	-0.036±0.009	-	-	-	-
τ^-	750.000	Ford (15)	0.2770±0.0035	0.020±0.010	-0.040±0.009	-	-	-	-
$\tau^+ + \tau^-$	1.500.000	Ford (15)	0.2737±0.0032	-	-	-	-	-	1.38
	1.500.000	Ford (15)	0.2877±0.0076	0.024±0.010	-0.039±0.009	-	-0.039 - 0.020	-0.021±0.016	1.26

(x) - The bidimensional fits to our data were performed removing the bins on the border of the Dalitz plot when the contour removes more than one third of the area of the bin.

(+) - Using only the y-projection.

where

$$x_1 = -\frac{3m_{\pi^+}^2}{2m_k Q} \tag{16}$$

$$y_1 = \frac{3}{2}\frac{1}{m_k Q}(m_k - m_3)^2 - \frac{3}{2}\frac{s_o}{m_k Q} - 1 \tag{17}$$

ii) between a and α:

$$a = \frac{x_2 \alpha}{1 + y_2 \alpha} \tag{18}$$

where

$$x_2 = 4\frac{m_k}{m_{\pi^+}^2}\frac{Q}{3} \tag{19}$$

$$y_2 = 2\frac{m_k}{m_{\pi^+}^2}\left(\frac{2}{3}Q - T\right) \tag{20}$$

iii) between g and α:

$$g = \frac{x_3 \alpha}{1 + y_3 \alpha} \tag{21}$$

where

$$x_3 = x_1 x_2 = -2 \tag{22}$$

$$y_3 = x_2 y_1 + y_2 \tag{23}$$

Numerical values of the coefficients x_i and y_i are given in Table VIII, which also lists some kinematical values of the various 3π decays. Using equations (15-23) we have computed from the published values the a, g and α coefficients.

Table IX gives a summary of the present situation of $K \to 3\pi$ decay. In particular it gives the number of events, the type of fit performed by the author and the coefficients a, g and α computed by us.

The average values of the g_{τ^+} and g_{τ^-} are equal within errors, in agreement with CP conservation.

TABLE VIII

Some numerical values in $K \to 3\pi$ decays.

	$K^{\pm} \to \pi^{\pm} + \pi^{\pm} + \pi^{\mp}$	$K^{\pm} \to \pi^{\pm} + \pi^{o} + \pi^{o}$	$K_L^o \to \pi^+ + \pi^- + \pi^o$
m_k (GeV)	0.49371	0.49371	0.4977
$m_{1,2}$ (GeV)	0.139569	0.134964	0.139569
m_3 (GeV)	0.139569	0.139569	0.134964
Q (GeV)	0.07500	0.08421	0.08360
$T_o = T_{3max}$ (GeV)	0.04810	0.05322	0.05391
S_o $(GeV)^2$	0.10073	0.09989	0.10163
$\mu = m_k / m^2_{\pi^+}$ $(GeV)^{-1}$	25.34510	25.34510	25.54993
x_1	-0.7890	-0.7027	-0.7022
y_1	0.	-0.07901	0.07967
x_2	2.5346	2.8458	2.8479
y_2	$(= y_3)$	0.14791	0.09326
x_3	-2.	-2.	-2.
y_3	0.09626	-0.07694	0.32015

The average values of the g and α coefficients are:

$$g_\tau = -0.213 \pm 0.002 \qquad \alpha_\tau = 0.1075 \pm 0.001$$

$$g_{\tau'} = 0.526 \pm 0.015 \qquad \alpha_{\tau'} = -0.268 \pm 0.008$$

$$g_{ko} = 0.593 \pm 0.008 \qquad \alpha_{ko} = -0.271 \pm 0.003$$

from which:

$$-\frac{g_{\tau'}}{2g_\tau} = 1.235 \pm 0.035 \qquad -\frac{\alpha_{\tau'}}{2\alpha_\tau} = 1.245 \pm 0.035$$

$$-\frac{g_{ko}}{2g_\tau} = 1.390 \pm 0.025 \qquad -\frac{\alpha_{ko}}{2\alpha_\tau} = 1.260 \pm 0.015$$

$$\frac{g_{\tau'}}{g_{ko}} = 0.887 \pm 0.026 \qquad \frac{\alpha_{\tau'}}{\alpha_{ko}} = 0.989 \pm 0.030$$

TABLE IX

Compilation of experimental results on the slopes a, g and α. The table gives the explicit form for $|M|^2$ used by the author in fitting the $K \to 3\pi$ decays and the resulting lowest order coefficient. The values a, g and α have then been computed using formulae[15-23].

Reference	Number of events	Average momentum (GeV/c)	Fit to $\|M\|^2$	Reference value	a	g	α
τ^+							
This exper.	27.940	0.14-1.5	$1+ay$	0.236 ±.013	0.236 ±.013	-0.186 ±.010	0.094 ±.005
Huetter (9)	3.587	at rest	$1+a'\mu Qy$	0.110 ±.020	0.209 ±.038	-0.165 ±.030	0.083 ±.015
Zinchenko (10)	5.428	at rest	$1+ay$	0.280 ±.030	0.280 ±.030	-0.221 ±.024	0.112 ±.012
Butler (11)	9.994	0.2-1.4	$1+ay$	0.288 ±.015	0.288 ±.015	-0.227 ±.012	0.115 ±.006
Ford (1)	750.000	3.0	$1+ay+bx^2+cy^2$	0.2734±.0035	0.2734±.0035	-0.2157±.0028	0.1090±.0014
Hoffmaster (14)	39.819	at rest	$1+a'\mu Qy$	0.134 ±.005	0.255 ±.009	-0.201 ±.007	0.102 ±.004
Average						-0.212 ±.002	0.107 ±.001
τ^-							
Ferro-Luzzi (8)	1.347	0.3-0.8	$1+ay$	0.280 ±.045	0.280 ±.045	-0.221 ±.035	0.112 ±.018
Moscoso (12)	5.121	0.7-1.2	$1+a'\mu Qy$	0.127 ±.015	0.242 ±.028	-0.191 ±.022	0.096 ±.011
Mast (13)	50.919	0.2-0.5	$1+ay$	0.247 ±.009	0.247 ±.009	-0.195 ±.007	0.098 ±.004
Ford (15)	750.000	3.0	$1+ay+bx^2+cy^2$	0.2770±.0035	0.2770±.0035	-0.2185±.0028	0.1104±.0014
Lucas (16)	81.000	0.4	$1+ay$	0.252 ±.011	0.252 ±.011	-0.199 ±.009	0.100 ±.004
Average						-0.214 ±.002	0.108 ±.001
τ'^+							
Kalmus (17)	1.792	at rest	$\left[1+g(s_3-s_o)/m_\pi^2\right]^2$	0.24 ±.02	-0.722±.064	0.480 ±.040	-0.24 ±.028
Bisi (18)	1.874	at rest	$1+\alpha'\mu(2T_3-T_o)$	-0.58 ±.12	-0.86 ±.19	0.57 ±.11	-0.29 ±.06
Davison (19)	4.048	at rest	$1+g(s_3-s_o)/m_\pi^2$	0.516±.018	-0.779±.029	0.516 ±.018	-0.263 ±.013
Aubert (20)	1.365	at rest	$[1+ay]^2$	-0.451±.028	-0.902±.056	0.592 ±.034	-0.303 ±.025
Average						0.526 ±.015	-0.268 ±.008
$K_L^o \to \pi^+\pi^-\pi^o$							
Hopkins (22)	1.198	2.0	$1+2\alpha\mu(2T_3-T_o)$	-0.294±.018	-0.861±.054	0.649±.044	-0.294±.018
Nefkens (21)	1.350	0.4-4.	$1+2\bar{\alpha}\mu(2T_3-\frac{2}{3}Q)$	-0.204±.025	-0.581±.071	0.428±.055	-0.200±.024
Basile (23)	2.446	0.25	$1+2\alpha\mu(2T_3-T_o)$	-0.188±.020	-0.545±.059	0.400±.045	-0.188±.020
Albrow (24)	29.000	3.	$1+a'(Q/M_k)y$	-5.14 ±.09	-0.863±.015	0.651±.012	-0.295±.005
Buchanan (25)	36.000	5.	$1+2\bar{\alpha}\mu(2T_3-\frac{2}{3}Q)+\beta\mu^2(2T_3-\frac{2}{3}Q)^2$	-0.257±.005	-0.732±.014	0.546±.012	-0.251±.005
Smith (26)	4.200	1.5	$1+2\alpha\mu(2T_3-T_o)$	-0.297±.024	-0.870±.072	0.656±.058	-0.297±.024
Krenz (27)	1.486	0.9	$1+2\alpha\mu(2T_3-T_o)$	-0.277±.018	-0.810±.054	0.608±.043	-0.277±.018
Average						0.593±.008	-0.271±.003

These values do not agree with the values of 1 predicted by the $\Delta I = 1/2$ selection rule.

ACKNOWLEDGEMENTS. -

The authors wish to acknowledge the contribution of many members of the CERN staff to the taking of the film and that of other members of the BGRT Collaboration to the analysis of the film. They express their appreciation to the scanning, measuring, and computing staff of their respective laboratories. The Glasgow group wishes to thank the Science Research Council for its support.

REFERENCES. -

(1) - G. Giacomelli, P. Lugaresi-Serra, G. Mandrioli, A.M. Rossi, F. Griffiths, I.S. Hughes, D.A. Jacobs, R. Jennings, B.C. Wilson, G. Ciapetti, V. Costantini, G. Martellotti, D. Zanello, E. Castelli and M. Sessa, Nuclear Phys. B20, 301 (1970).
(2) - G. Giacomelli, P. Lugaresi-Serra, F. Mercatali, A. Minguzzi-Ranzi, A.M. Rossi, F. Griffiths, A.A. Hirata, I.S. Hughes, R. Jennings, B.C. Wilson, G. Ciapetti, P. Guidoni, G. Martellotti, A. Nappi, D. Zanello, E. Castelli, P. Poropat and M. Sessa, Nuclear Phys. B37, 577 (1972).
(3) - S. Focardi, A. Minguzzi-Ranzi, L. Monari, G. Saltini, P. Serra, T.A. Filippas, and V.P. Henry, Phys. Letters B24, 314 (1967).
(4) - V. Cameron, A.A. Hirata, R. Jennings, W.T. Morton, E. Cazzoli, G. Giacomelli, P. Lugaresi-Serra, G. Mandrioli, A. Minguzzi-Ranzi, E. Castelli, M. Furlan, P. Poropat, C. Omero and M. Sessa, K^+p scattering from 130 to 755 MeV/c, Nuclear Phys., to be published.
(5) - R.H. Dalitz, Phil. Mag. 44, 1068 (1953).
(6) - R.H. Dalitz, Rept. Progr. Phys. 20, 163 (1957).
(7) - E. Fabri, Nuovo Cimento 11, 479 (1954).
(8) - M. Ferro-Luzzi, D.H. Miller, J.J. Murray, A.H. Rosenfeld and R.D. Tripp, Nuovo Cimento 22, 1087 (1961).
(9) - T. Huetter, S. Taylor, E.L. Koller, P. Stamer and J. Grauman, Phys. Rev. 140, B655 (1965).
(10) - B. Zinchenko, Thesis, Rutgers University (1967).
(11) - W.R. Butler, R.W. Bland, G. Goldhaber, S. Goldhaber, A.A. Hirata, T. O'Halloran, G.H. Trilling and C.G. Wohl, UCRL-18420 (1968).
(12) - M.L. Moscoso, Thesis, University of Paris-Orsay (1968).
(13) - T.S. Mast, L.K. Gershwin, M. Alston-Garnjost, R.O. Bangerter, A.

Barbaro-Galtieri, J.J. Murray, F.T. Solmitz and R.D. Tripp, Phys. Rev. 183, 1200 (1969).

(14) - S. Hoffmaster, E.L. Koller, S. Taylor, L. Romano, D. Pandoulas, O. Raths, J. Grauman, P. Stamer, A. Kanofsky and V. Mainkar, Nuclear Phys. B36, 1 (1972).

(15) - W.T. Ford, P.A. Pirouè, R.S. Remmel, A.J.S. Smith and P.A. Souder, Phys. Letters 38B, 335 (1972).

(16) - P.W. Lucas, H.D. Taft and W.J. Willis, Phys. Rev. D8, 719 (1973).

(17) - G.E. Kalmus, A. Kernan, R.T. Pu, W.M. Powell and R. Dowd, Phys. Rev. Letters 13, 99 (1964).

(18) - V. Bisi, G. Borreàni, R. Cester, A. De Mazo-Trabucco, M. Ferrero, C. Garelli, A. Chiesa, B. Quassiati, R. Rinaudo, M. Vigone and A. Verbrouck, Nuovo Cimento 35, 768 (1965).

(19) - D. Davison, R. Bacastow, W.N. Barkas, D.A. Evans, S.Y. Fung, L.E. Porter, R.T. Poe and D. Greiner, Phys. Rev. 180, 1333 (1969).

(20) - B. Aubert, P. Heusse, C. Pascaud, J.P. Vialle, D. Bertrand, P. Vilain, V. Brisson and P. Petiau, Nuovo Cimento 12A, 509 (1972).

(21) - B.M.K. Nefkens, A. Abashian, R.J. Abrams, D.W. Carpenter, G.P. Fisher and J.H. Smith, Phys. Rev. 157, 1233 (1967).

(22) - H.W.K. Hopkins, T.C. Bacon and F.R. Eisler, Phys. Rev. Letters 19, 185 (1967).

(23) - P. Basile, J.W. Cronin, B. Thevenet, R. Turlay, S. Zylberaich and A. Zylberztein, Phys. Letters 28B, 58 (1968).

(24) - M.G. Albrow, D. Aston, D.P. Barber, L. Bird, R.J. Ellison, C. Halliwell, R.E.H. Jones, A.D. Kanaris, F.K. Loebinger, P.G. Murphy, M. Strong, J. Walters, A.J. Wynroe, D.D. Yovanovic and R.F. Templeman, Phys. Letters 33B, 516 (1970).

(25) - C.D. Buchanan, D.J. Drickey, F.D. Rudnick, P.F. Shepard, D.R. Stork, H.K. Ticho, C. -Y. Chien, B. Cox, L. Ettlinger, L. Resvanis, R.A. Zdanis, E. Dally, E. Seppi and P. Innocenti, Phys. Letters 33B, 623 (1970).

(26) - R.C. Smith, L. Wang, M.C. Whatley, G.T. Zorn and J. Hornobostel, Phys. Letters 32B, 133 (1970).

(27) - W. Krenz, H.W.K. Hofkins, G.R. Evans, J. Muir and J.J. Peach, Lett. Nuovo Cimento 4, 213 (1972).

(28) - Particle Data Group, Review of particle properties, Rev. Mod. Phys. 45, n. 2, part. 2 (1973).